Analysis of Distance/Similarity Measures for Diffusion Tensor Imaging

T.H.J.M. Peeters, P.R. Rodrigues, A. Vilanova, and B.M. ter Haar Romeny

Department of Biomedical Engineering, Eindhoven University of Technology,
WH 2.103, 5600 MB Eindhoven, The Netherlands
{T.H.J.M.Peeters, P.R.Rodrigues, A.Vilanova, B.M.terHaarRomeny}@tue.nl

Summary. Many different measures have been proposed to compute similarities and distances between diffusion tensors. These measures are commonly used for algorithms such as segmentation, registration, and quantitative analysis of Diffusion Tensor Imaging data sets. The results obtained from these algorithms are extremely dependent on the chosen measure. The measures presented in literature can be of complete different nature, and it is often difficult to predict the behavior of a given measure for a specific application. In this chapter, we classify and summarize the different measures that have been presented in literature. We also present a framework to analyze and compare the behavior of the measures according to several selected properties. We expect that this framework will help in the initial selection of a measure for a given application and to identify when the generation of a new measure is needed. This framework will also allow the comparison of new measures with existing ones.

1 Introduction

Diffusion tensor imaging (DTI) is a magnetic resonance technique that measures the diffusion of water in tissue. If the tissue is fibrous, the water molecules diffuse more in directions along the fibers than perpendicular to them. To capture the anisotropic behavior, the diffusion is often represented by a symmetric positive definite second-order tensor. Using tractography (e.g., see Vilanova et al. [15]) it is possible to reconstruct connections in the brain or the fibrous structure of muscle tissue such as the heart (e.g., see Zhukov et al. [19]). In several applications, for example, comparison between subjects, it is interesting to segment structures with a higher level of meaning, for example, white matter bundles, that is [14, 16, 20], and also to register different DTI data sets [1, 10, 18]. It is often also necessary to derive statistical properties of diffusion tensors (DTs) to identify differences, for example, between healthy and pathology areas [11].

In all the previous methods, it is often needed to define the difference between diffusion tensors, that is, to compare diffusion tensors. In segmentation and registration, similarity measures are applied to match DTs in voxels in a certain region, and between regions of different data sets. In quantitative analysis or DT statistics, distance or similarity measures of DTs in neighboring voxels can be used to classify the amount of variability in a selected voxel [13] or volume of interest. The results of these applications are highly dependent on the choice of measure.

Alexander et al. [1] listed several measures and analyzed their results for segmentation. However, since then, various people have introduced new measures for comparing DTs. These measures are of different nature and it is very difficult to predict which measure will give better or similar results. There exist numerous measures, but to our best knowledge, there is no overview that compares and classifies them in a structured way. This comparison can help to support researchers in choosing a measure, and being able to predict the behavior of the measures for their concrete application.

In this chapter, we provide this analysis and improve the intuition in the behavior of the measures. The intrinsic characteristics of a measure are analyzed without having a specific application in mind. This allows an evaluation of the nature of the measure in itself. It is out of the scope of this chapter to make an application-oriented analysis, (e.g., finding the best measure for DTI adult brain registration). However, this chapter aims to help make a first selection of the possible measures that could be used for such application by looking at the characteristics of the problem and the characteristics of the measures. We expect that it will also help to identify when a new measure is necessary, and compare its behavior with existing ones.

First, we present the notations used in this paper. In Sect. 3, we describe the properties that will be used for the analysis of the measures. In Sect. 4, we give an overview of existing measures from literature. In Sect. 5, we explain how we evaluate the properties of the measures and show some simple results to illustrate our methods. Section 6 presents the results of the experiments. Finally, in Sect. 7, conclusions and summarized results are described.

2 Notation

We represent symmetric positive definite second-order tensors, Sym_3^+, by capital bold letters, for example, $\mathbb{D} \in Sym_3^+$. The scalar components of a tensor $\mathbb{D}$ are denoted by $\mathbb{D}_{ij}$:

$$\mathbb{D} = \begin{pmatrix} \mathbb{D}_{11} & \mathbb{D}_{12} & \mathbb{D}_{13} \\ \mathbb{D}_{12} & \mathbb{D}_{22} & \mathbb{D}_{23} \\ \mathbb{D}_{13} & \mathbb{D}_{23} & \mathbb{D}_{33} \end{pmatrix}$$

Eigenvalues of tensor $\mathbb{D}$ are $\lambda_1^{\mathbb{D}} \geq \lambda_2^{\mathbb{D}} \geq \lambda_3^{\mathbb{D}} \geq 0$ and the corresponding eigenvectors are $\overline{e}_1^{\mathbb{D}}$, $\overline{e}_2^{\mathbb{D}}$, and $\overline{e}_3^{\mathbb{D}}$. We denote the trace $(\sum_{i=1}^{3} \mathbb{D}_{ii}) = (\sum_{i=1}^{3} \lambda_i^{\mathbb{D}})$ of $\mathbb{D}$ with $\mathrm{tr}(\mathbb{D})$. The determinant of $\mathbb{D}$ will be denoted by $\det(\mathbb{D})$.

With *measure* we refer to a function m that has two tensors $\mathbb{A}$, $\mathbb{B}$ as input, and returns a nonnegative scalar value:

$$m : Sym_3^+ \times Sym_3^+ \mapsto \mathbb{R}_0^+. \tag{1}$$

If a measure returns how similar $\mathbb{A}$ and $\mathbb{B}$ are, then we call the measure a *similarity measure*. If it returns how different $\mathbb{A}$ and $\mathbb{B}$ are, we call it a *distance measure*. We denote similarity measures with s and distance measures with d.

3 Properties

In this section, we present a list of properties that can be evaluated for the different measures. Diffusion tensors can be classified by their size, orientation, and shape. We evaluate the measures according to their sensitivity to changes in these properties. These changes are illustrated in Fig. 1. We also include as a property how robust the measures are to noise, and the fact that a measure is a metric or not.

3.1 Size

We understand as the size of a DT the mean diffusivity $MD = \mathrm{tr}(\mathbb{D})/3$. This is illustrated in Fig. 1(a). We consider a measure to be size-invariant if it is uniform scaling invariant, that is, if it fulfills

$$m(s\mathbb{A}, t\mathbb{B}) = m(\mathbb{A}, \mathbb{B}), \tag{2}$$

where s and t are scalar values.

3.2 Orientation

A measure m is rotation invariant if the value of m does not change when the input tensors are rotated:

$$m(R^T\mathbb{A}R, P^T\mathbb{B}P) = m(\mathbb{A}, \mathbb{B}), \tag{3}$$

where R and P are rotation matrices. The orientation invariance can be divided into two. One is whether the measure is sensitive, in general, to the difference in orientation between tensors. Orientation changes are illustrated in Fig. 1(b, c).

The other invariance included in the previous is invariance to image rotation. If we define a DTI image as $f : \mathbb{R}^3 \mapsto Sym_3^+$ in most of the cases, we want that our measure is invariant to rigid body transformations of f (i.e., rotation and translation). In the case of DTI images, the image transformation also has to be applied to the tensor. From these transformations the rotation is the only one that affects the tensor. Being invariant to image rotation means that we want to fulfill (3) when $R = P$. If the image f is transformed with other transformation (e.g., nonuniform scaling, skewing), it is not clear how this should affect the tensor and therefore we consider it out of the scope of this chapter.

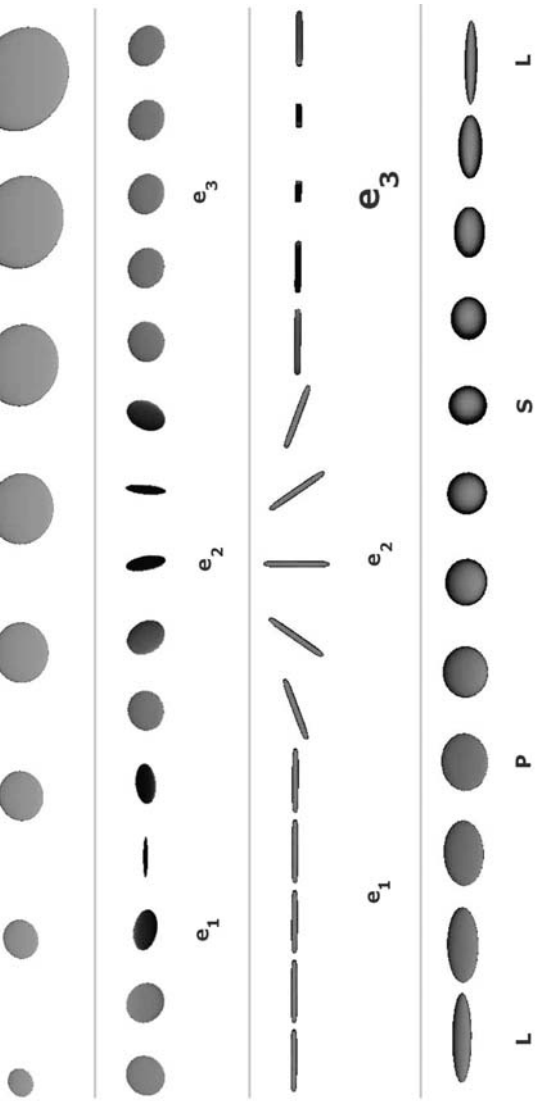

Fig. 1. Ellipsoidal glyphs showing smoothly varying DTs. (**a**) A planar-shaped DT where the size is increased smoothly, that is, MD increases; (**b**) a planar-shaped DT is rotated smoothly, until π, first around $\bar{e}_1$, then around $\bar{e}_2$, and finally around $\bar{e}_3$; (**c**) a linear-shaped DT is rotated smoothly as in (b); (**d**) DTs where the shape changes from linear (L), to planar (P), to spherical (S), and back to linear (L)

3.3 Shape

The shape of a tensor can be defined as *linear*, *planar*, *spherical*, or as an interpolation between these types. The shape is given by the ratio between the different eigenvalues. A graphical representation of different tensor shapes is shown in Fig. 1(d). A measure m is shape-invariant if the value of $m(\mathbb{A}, \mathbb{B})$ does not change when changing the shape (i.e., the ratio between eigenvalues) of $\mathbb{A}$, $\mathbb{B}$, or both.

3.4 Robustness

Measures are never completely invariant to noise. However, if small changes in the input produce small changes in output, then we consider the measures to be robust under noise. Therefore, we can define

$$|m(\mathbb{A} + \mathbb{E}1, \mathbb{B} + \mathbb{E}2) - m(\mathbb{A}, \mathbb{B})| \leq \varepsilon, \tag{4}$$

where ε is a very small scalar value and the components $\mathbb{E}\{1,2\}_{ij}$ of $\mathbb{E}\{1,2\} \in Sym_3$ are also very small values.

3.5 Metric

A distance measure d is a semi-metric if, for two tensors $\mathbb{A}$ and $\mathbb{B}$, it satisfies the following conditions:

$$\mathbb{A} = \mathbb{B} \Leftrightarrow d(\mathbb{A}, \mathbb{B}) = 0 \tag{5}$$

$$d(\mathbb{A}, \mathbb{B}) = d(\mathbb{B}, \mathbb{A}). \tag{6}$$

Condition (5) is important because it allow us to distinguish between equal and nonequal tensors. Condition (6) is necessary if we do not want the results to depend on the order in which we deal with the DTs in a volume. If the measure has to be a Riemannian metric, it also has to fulfill, for infinitesimally close $\mathbb{A}$ and $\mathbb{B}$,

$$d(\mathbb{A}, \mathbb{B}) \leq d(\mathbb{A}, \mathbb{C}) + d(\mathbb{C}, \mathbb{B}). \tag{7}$$

Condition (7) is important in applications where you need to take the mean or do interpolation between tensors [2, 12].

4 Measures

In this section, we present a classification of similarity and distance measures for diffusion tensors (DTs) that have been used in literature. This classification is based on the nature of the derivation of the measure: measures based on scalar indices; measures that make use of the angles between eigenvectors; measures based in linear algebra; measures based on imposing the preservation of positive definiteness of the tensor, that is, Riemannian geometry; measures

considering the DTs as a representation of a probability density function and, finally, measures that combine different measures from the previous classes.

4.1 Scalar Indices

Given a scalar index $g : Sym_3^+ \mapsto \mathbb{R}_0^+$, the simplest way to obtain a difference between two DTs $\mathbb{A}$ and $\mathbb{B}$ is by using the absolute difference $|g(\mathbb{A}) - g(\mathbb{B})|$ of the scalar index of the two tensors. There exist numerous scalar indices that can be chosen for g. Two well-known examples are fractional anisotropy (FA) and linear anisotropy (C_l). For a selection of scalar indices, see Table 1 and refer to Westin et al. [17] and Vilanova et al. [15]. These indices reduce the 6D information in a DT to a scalar value. In the computation of the scalar value, only the rotationally invariant eigenvalues of the tensors are used, thus they do not depict the directional variation of the diffusion anisotropy. The measures created from scalar indices will be denoted by ds, with the short name of the index as subscript, for example, ds_{FA}, ds_{C_l}, ds_{MD}. Thus

$$ds_{FA}(\mathbb{A}, \mathbb{B}) = |FA(\mathbb{A}) - FA(\mathbb{B})|. \tag{8}$$

When using ds, a lot of information is lost. Each DT is represented by one scalar value, while six scalar values are needed to represent the full DT. Thus, the measures based on scalar indices can be very limited.

More scalar indices can be derived from tensors. For example, several DTI literature recognized the benefit of *tensor invariants* as measure of the diffusion tensor shape that do not require diagonalization. Kindlmann [8] used these invariants, like the mean, variance, and skewness, which are invariant to rotation, to measure the shape gradients in tensor fields. However, using them for constructing a distance measure will give similar results to ds and will not solve the problem that just one aspect is being shown. Thus, we do not treat them separately here.

Table 1. Scalar indices for diffusion tensors [15, 17]

Name	Abbrev.	Equation
Mean diffusivity	MD	$= \mathrm{tr}(\mathbb{D})/3 = (\lambda_1 + \lambda_2 + \lambda_3)/3$
Fractional anisotropy	FA	$= \frac{\sqrt{(\lambda_1-\lambda_2)^2+(\lambda_2-\lambda_3)^2+(\lambda_1-\lambda_3)^2}}{\sqrt{2(\lambda_1^2+\lambda_2^2+\lambda_3^2)}}$
Relative anisotropy	RA	$= \frac{\sqrt{(\lambda_1-\lambda_2)^2+(\lambda_2-\lambda_3)^2+(\lambda_1-\lambda_3)^2}}{\sqrt{2}(\lambda_1+\lambda_2+\lambda_3)}$
Linear anisotropy	c_l	$= (\lambda_1 - \lambda_2)/(\lambda_1 + \lambda_2 + \lambda_3)$
Planar anisotropy	c_p	$= 2(\lambda_2 - \lambda_3)/(\lambda_1 + \lambda_2 + \lambda_3)$
Isotropy	c_s	$= 3\lambda_3/(\lambda_1 + \lambda_2 + \lambda_3)$
Volume Ratio	VR	$= \lambda_1\lambda_2\lambda_3/MD^3$

4.2 Angular Difference

Angular difference d_{ang_i} of the main eigenvectors $\overline{e}_i^{\mathbb{D}}$ is often used as a distance between tensors that measures change in orientation [21]:

$$d_{ang_i}(\mathbb{A}, \mathbb{B}) = \arccos(\overline{e}_i^{\mathbb{A}} \cdot \overline{e}_i^{\mathbb{B}}). \tag{9}$$

Using d_{ang_1} only makes sense for tensors where the diffusion is mainly linear. If the tensors have planar shape then d_{ang_3} can be used. For tensors with spherical shape, any d_{ang_i} can be considered random and should not be used.

4.3 Linear Algebra

A class of measures deal with the diffusion tensors components as vector elements. A typical distance measure is the L^n-norm of the componentwise difference of two vectors:

$$d_{Ln}(\mathbb{A}, \mathbb{B}) = \sqrt[n]{\sum_{i=1}^{3}\sum_{j=1}^{3}(\mathbb{A}_{ij} - \mathbb{B}_{ij})^n}. \tag{10}$$

In DTI literature, the L^2-norm, d_{L2}, is most commonly used for computing a distance measure (see Batchelor et al. [4]); therefore, we only treat d_{L2} in this chapter. d_{L2} is the same as the *Frobenius distance* [21], which is computed using $d_F(\mathbb{A}, \mathbb{B}) = \sqrt{\mathrm{tr}((\mathbb{A} - \mathbb{B})^2)}$.

One can also compute the *scalar product* of two tensors by summing the products of components of the tensors [1]. The result can be used as a similarity measure s_{sp}:

$$s_{sp}(\mathbb{A}, \mathbb{B}) = \sum_{i=1}^{3}\sum_{j=1}^{3}\mathbb{A}_{ij}\mathbb{B}_{ij}. \tag{11}$$

Measures s_{sp} and d_{Ln} treat the DTs as simple vectors and ignore the matrix or tensor nature of them. Another class of measures use the fact that we have matrices. Pierpaoli and Basser [13] propose to use the sum of the squared vector dot products of the eigenvectors weighted by the product of the eigenvalues as a tensor scalar product [7]: s_{tsp} includes the colinearity of the orientation of the tensors weighted by its eigenvalues. The value is maximized if the tensors are aligned.

$$s_{tsp}(\mathbb{A}, \mathbb{B}) = \sum_{i=1}^{3}\sum_{j=1}^{3}\lambda_i^{\mathbb{A}}\lambda_j^{\mathbb{B}}(\overline{e}_i^{\mathbb{A}}\overline{e}_j^{\mathbb{B}})^2. \tag{12}$$

This measure is also called tensor dot product [3]. It is used to construct the *lattice index*, which we show in Sect. 4.6. Jonasson et al. [7] use the normalized

tensor scalar product s_{ntsp} in order to make it invariant to scaling of the tensors:

$$s_{ntsp}(\mathbb{A}, \mathbb{B}) = \frac{s_{tsp}(\mathbb{A}, \mathbb{B})}{\text{tr}(\mathbb{A})\text{tr}(\mathbb{B})}. \tag{13}$$

Instead of applying the aforementioned measures to the tensors directly, they can also be applied to the *deviatoric* of the DTs (see, e.g., [1]). The deviatoric $\tilde{\mathbb{D}}$ of tensor $\mathbb{D}$ represents the nonisotropic part of $\mathbb{D}$. It expresses just the shape and orientation of the DT, independent of the size. It can be computed as follows:

$$\tilde{\mathbb{D}} = \mathbb{D} - \frac{1}{3}\text{tr}(\mathbb{D})\mathbb{I}, \tag{14}$$

where $\mathbb{I}$ is the identity matrix. Note that $\tilde{\mathbb{D}}$ is not a positive definite tensor everywhere. This means that it can have negative eigenvalues, and some of the measures will also give negative values.

4.4 Riemannian Geometry

If we constrain the matrices to positive definite matrices, we get another class of measures based on Riemannian geometry. Batchelor et al. [4] introduced a geometric-based distance d_g that measures the distance between two tensors in the space of positive definite tensors:

$$d_g(\mathbb{A}, \mathbb{B}) = N(\mathbb{A}^{-\frac{1}{2}}\mathbb{B}\mathbb{A}^{-\frac{1}{2}}), \tag{15}$$

where

$$N(\mathbb{D}) = \sqrt{\sum_{i=1}^{3}(\log(\lambda_i^{\mathbb{D}}))^2}. \tag{16}$$

This measures the distances along geodesics in the manifold of symmetric positive defined matrices. Additionally, it is invariant to any linear change of coordinates. Pennec et al. [12] introduce a similar framework with the same distance measure, and extend it with methods for filtering and regularization of tensor fields.

Arsigny et al. [2] introduce a new *Log-Euclidian* framework. It has similar theoretical properties as Pennec et al.'s framework, but with simpler and faster calculations. They derive the following Log-Euclidian distance measure d_{LE}:

$$d_{LE}(\mathbb{A}, \mathbb{B}) = \sqrt{\text{tr}((\log(\mathbb{A}) - \log(\mathbb{B}))^2)}. \tag{17}$$

This measure is equivalent to the d_{L2} of the logarithm of the matrices. The details of its computation and derivation can be found in Arsigny et al. [2].

4.5 Statistics

A diffusion tensor can be interpreted as the covariance matrix of a Gaussian distribution describing the local diffusion. Thus, a natural family of dissimilarity measures between DTs would be the statistical divergence that

measures the overlapping of probability density functions. Given a diffusion tensor $\mathbb{D}$, the displacement $\mathbf{r}$ of water molecules at time t is a random variable with the following probability density function (pdf):

$$p(\mathbf{r}|t,\mathbb{D}) = \frac{1}{\sqrt{(2\pi)^n \det(2t\mathbb{D})}} \mathrm{e}^{-(\mathbf{r}^T D^{-1}\mathbf{r})/(4t)},$$

where n is the dimensionality of the square matrix $\mathbb{D}$.

Wang and Vemuri [16] proposed to use the square-root of the J-divergence (symmetrized Kullback–Leibler) as a new definition of DT distance d_{KL}:

$$d_{KL}(\mathbb{A},\mathbb{B}) = \frac{1}{2}\sqrt{\mathrm{tr}(\mathbb{A}^{-1}\mathbb{B} + \mathbb{B}^{-1}\mathbb{A}) - 2n}, \tag{18}$$

where the dimensionality n is 3 for DTs.

In probability theory, class separability can be measured by the overlap between the corresponding pdfs. Therefore, the overlap of pdfs can also be used as a similarity measure between tensors. The calculation of the overlap cannot be done analytically and often approximations are being used. The Chernoff bound [6] gives us the upper bound of the probability error, $P(error)$, of a Bayesian classifier for two classes, w_1 and w_2, given their pdfs $P(w_1)$ and $P(w_2)$. For normal distributions we have

$$P(error) \leq P^{\beta}(w_1)P^{1-\beta}(w_2)\mathrm{e}^{-k\beta},$$

where β is a parameter that needs to be optimized to find the Chernoff bound. A special case is the Bhattacharyya bound where $\beta = 1/2$. This bound is never looser than the optimal Chernoff bound and can be directly calculated. For DTs, it becomes the following similarity measure:

$$s_{Bhat}(\mathbb{A},\mathbb{B}) = \mathrm{e}^{-\frac{1}{2}ln\left(\frac{\det(\frac{\mathbb{A}+\mathbb{B}}{2})}{\sqrt{\det(\mathbb{A})\det(\mathbb{B})}}\right)}. \tag{19}$$

4.6 Composed

As mentioned in Sect. 4.1, each scalar measure in itself can give very limited information of the difference between DTs (e.g., FA just gives information about the anisotropy). Usually, a measure that reflects the changes of a combination of these properties is necessary. Therefore, several authors have tried to combine simple measures to obtain a more complete measure. Often, the measures that are combined have quite different natures and therefore ad hoc normalizations and weighting factors are needed.

Pollari et al. [10] introduced shape-dependent similarity measures, which are used depending on the DT shape:

$$
\begin{aligned}
s_l(\mathbb{A},\mathbb{B}) &= |\overline{e}_1^{\mathbb{A}} \cdot \overline{e}_1^{\mathbb{B}}| = \cos(d_{ang_1}(\mathbb{A},\mathbb{B})) \\
s_p(\mathbb{A},\mathbb{B}) &= |\overline{e}_3^{\mathbb{A}} \cdot \overline{e}_3^{\mathbb{B}}| = \cos(d_{ang_3}(\mathbb{A},\mathbb{B})) \\
s_s(\mathbb{A},\mathbb{B}) &= 1 - \tfrac{|\mathrm{tr}(\mathbb{A})-\mathrm{tr}(\mathbb{B})|}{max(\mathrm{tr}(\mathbb{A}),\mathrm{tr}(\mathbb{B}),1)} \\
s_{T_2}(a,b) &= 1 - \tfrac{|g^a-g^b|}{max(g^a,g^b,1)},
\end{aligned}
$$

where a and b are the voxels with tensors $\mathbb{A}$ and $\mathbb{B}$. g^a, g^b are the grey-levels in a, b in the T_2 MRI data. Using s_{l,p,s,T_2}, Pollari et al. introduce a DT distance measure for registration of DTI brain datasets that looks at the overlap between diffusion shapes and weighs this with the most reliable information for that shape:

$$
\begin{aligned}
I(a,b) = \hat{c}_l^{\mathbb{A}}\hat{c}_l^{\mathbb{B}} s_l(\mathbb{A},\mathbb{B}) + \hat{c}_p^{\mathbb{A}}\hat{c}_p^{\mathbb{B}} s_p(\mathbb{A},\mathbb{B}) + \\
\gamma * \hat{c}_s^{\mathbb{A}}\hat{c}_s^{\mathbb{B}} \left(s_s(\mathbb{A},\mathbb{B}) + s_{T_2}(a,b)\right)/2,
\end{aligned} \tag{20}
$$

where γ is $\frac{1}{2}$ in all of their experiments because they want to give less weight to isotropic voxels. The anisotropy measures are defined as $\hat{c}_l = \frac{\lambda_1-\lambda_2}{\lambda_1}$, $\hat{c}_p = \frac{\lambda_2-\lambda_3}{\lambda_1}$, $\hat{c}_s = \frac{\lambda_3}{\lambda_1}$, which is a variation of the measures proposed by Westin [17] listed in Table 1. Because we are analyzing measures for DTs only, in Sect. 6 we use a modified similarity measure s_{pnl} that disregards the s_{T_2} term in (20):

$$
\begin{aligned}
s_{pnl}(\mathbb{A},\mathbb{B}) = \hat{c}_l^{\mathbb{A}}\hat{c}_l^{\mathbb{B}} s_l(\mathbb{A},\mathbb{B}) + \hat{c}_p^{\mathbb{A}}\hat{c}_p^{\mathbb{B}} s_p(\mathbb{A},\mathbb{B}) + \\
\gamma * \hat{c}_s^{\mathbb{A}}\hat{c}_s^{\mathbb{B}} s_s(\mathbb{A},\mathbb{B}).
\end{aligned} \tag{21}
$$

We also use $\gamma = \frac{1}{2}$, although a more precise analysis, of the robustness of this measure to the changes of gamma, would be needed.

Pierpaoli and Basser [13] introduced the *lattice index* as an intervoxel anisotropy measure that takes the DTs in neighboring voxels into account. For the computation of the lattice index they defined a measure s_{LI} that gives a similarity between two tensors:

$$
s_{LI}(\mathbb{A},\mathbb{B}) = \frac{\sqrt{3}}{\sqrt{8}} \frac{\sqrt{s_{tsp}(\tilde{\mathbb{A}},\tilde{\mathbb{B}})}}{\sqrt{s_{tsp}(\mathbb{A},\mathbb{B})}} + \frac{3}{4} \frac{s_{tsp}(\tilde{\mathbb{A}},\tilde{\mathbb{B}})}{\sqrt{s_{tsp}(\mathbb{A},\mathbb{A})}\sqrt{s_{tsp}(\mathbb{B},\mathbb{B})}}, \tag{22}
$$

with s_{tsp} as defined in (12) and $\tilde{\mathbb{A}}, \tilde{\mathbb{B}}$ as in (14). Because $s_{tsp}(\tilde{\mathbb{A}}, \tilde{\mathbb{B}})$ can be negative, s_{LI} can give negative or imaginary values, which do not fulfill the basic description of a measure as we defined it. Therefore, we do not use s_{LI} in further analysis.

5 Methods

For analyzing the properties of the measures, we want to show the behavior of each measure for the different properties in a global way. So, we show the results of each measure for sets of pairs of DTs where one property is changed. We change each property gradually and analyze the behavior of the measures.

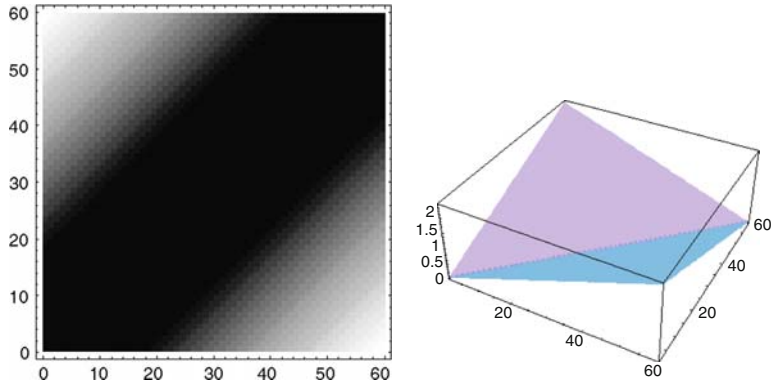

(a) (b)

Fig. 2. Size comparison plot of ds_{MD} for tensors with planar shape. On the axes from left to right, and from bottom to top, the size of the tensors increase while the shape and orientation are invariant. See Fig. 1(a). (**a**) A grey-value plot; (**b**) The height field

To do this analysis, we use plots as shown in Fig. 2. The axes of the plots have smoothly varying DTs and in the plot we show the similarity or difference of corresponding DTs. In Fig. 2(a) the results of the measure are shown as a grey-scale image. Figure 2(b) shows the same results as a height field, which gives a more clear impression about the evolution of the measure.

Furthermore, we compared the different measures by means of the root mean square difference (RMSD) of their normalized results. This allows us to grasp the similarities between the measures.

5.1 Size

Size is simple to evaluate because it can be captured with only one scalar value (mean diffusivity MD, see Table 1). Figure 2 shows a size comparison plot for ds_{MD}. From left to right and bottom to top, we increase the size of the tensor by multiplying the eigenvalues of a base tensor with increasing values. This is illustrated in Fig. 1(a). It can be seen from Fig. 2 that tensors with the same size (on the diagonal of the plot) have zero distance, and tensors of which the sizes differ have larger distances. Some measures (e.g., ds_{FA}) are invariant to scaling. So this plot will not be used for those measures.

5.2 Orientation

For orientation, we consider the sensitivity of the measure to rotation of the tensors, that is, rotation around any axis. For tensors with linear shape, the measure should be invariant to rotations around $\overline{e}_1$. For tensors with planar shape, the measure should be invariant to rotations around $\overline{e}_3$. For tensors

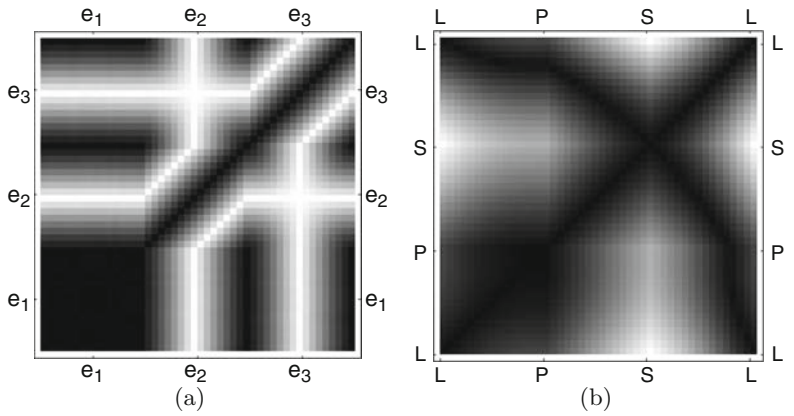

(a) (b)

Fig. 3. (**a**) Comparison plot for tensor with linear shape rotated around $\overline{e}_1$, $\overline{e}_2$, and $\overline{e}_3$ showing d_{ang_1}. See Fig. 1(c); (**b**) ds_{FA} comparison plot for tensors with shape changing from linear (L) to planar (P) to spherical (S) to linear (L). See Fig. 1(d)

with spherical shape, the measure should be invariant to any rotation. We created plots for multiple types (linear, planar, spherical) of tensors, where on both axes, we gradually rotate the tensor around $\overline{e}_1$ until π. Then, on the middle part of the horizontal and vertical axes of the plots, we rotate around $\overline{e}_2$ until π. Finally, in the top and right of the two axes we rotate around $\overline{e}_3$ until π. The tensors on the axes of the plots are illustrated in Figs. 1(b, c). Figure 3(a) shows results for d_{ang_1}. The tensor used for this image was linear. Thus, for rotation around $\overline{e}_1$, the distance does not change. This can be seen in the image because in the lower-left part, the distances stay zero. When rotating the tensor around $\overline{e}_2$ and $\overline{e}_3$, it can be seen that the distance between measures gradually increases for a rotation up to $\pi/2$ and then decreases again until it is zero at π.

Furthermore, we tested the rotation invariance of the measures to the situation when we rotate the volume. We did this by applying the same rotation to every tensor in a set, and then computing the RMSD of these results to the corresponding ones without rotation.

5.3 Shape

We consider that DTs can have linear, planar, or spherical shape or a shape that is a combination of these shapes. To study the behavior of the measure under changes in shape, we start with tensors that have linear shape, and then gradually change the shape to respectively planar, spherical, and back to linear. This is illustrated in Fig. 1(d). To make sure that we are only evaluating shape, we do not change the size and orientation of the tensors in the same plot. Results for ds_{FA} are shown in Fig. 3(b). As can be seen from the black

areas in the plot, which are not in the diagonal, tensors with different shapes can have the same value for FA. This is a known property of FA.

5.4 Robustness

From the results of the previous methods, we can derive whether a measure is sensitive to small changes in one of the properties. In addition, we introduce a small variation to the set of tensors in our experiments. To each component of the input tensors (on both axes) for making the size, shape, and orientation plots, we add a uniformly distributed random value. Then we analyze this robustness by computing the root mean square difference (RMSD) between the plots with and without the added noise. We consider the measures robust to noise if its plots do now show sharp changes or discontinuities, and the computed RMSDs are relatively small.

5.5 Metric

The conditions that need to be fulfilled for a measure to be a Riemannian metric can be derived from its definition. Thus, no experiments are needed to evaluate this property. However, we summarize whether the properties in (5)–(7) are fulfilled for each of the measures.

6 Experiments

In this section, we analyze and categorize behavior of the different measures using the methods described in the previous section. The behavior of the measures is summarized in Table 2.

6.1 Size

We can observe four different behaviors for the measures with respect to the size difference of the tensors. All scalar measures listed in Table 1, except MD, are invariant to scaling one or both input tensors with a scalar s. d_{ang_i}, s_{ntsp}, and s_{LI} are also invariant to scaling.

The measures ds_{MD} and d_{L2} show a behavior as illustrated in Fig. 2. The relation between the differences in size (MD) and the computed difference behaves as follows

$$d(\mathbb{A}, \mathbb{B}) = s \times |MD(\mathbb{A}) - MD(\mathbb{B})|, \tag{23}$$

where s is a scalar value. Scaling both $\mathbb{A}$ and $\mathbb{B}$ with a scalar value will change the outcome of ds_{MD} and d_{L2}, and so (24) is not valid for those measures if $\mathbb{A} \neq \mathbb{B}$:

$$d(s\mathbb{A}, s\mathbb{B}) = d(\mathbb{A}, \mathbb{B}). \tag{24}$$

This behavior is listed as *add* in Table 2.

Table 2. Overview of properties for similarity and distance measures for diffusion tensors

	Equation	Eqn	Cite	Size	Orientation	Shape	Robustness	Metric
ds_{FA}	$\lvert FA(\mathbb{A}) - FA(\mathbb{B})\rvert$	(8)	[17]	Invariant	Invariant	Not good	Shape only	No
ds_{MD}	$\lvert MD(\mathbb{A}) - MD(\mathbb{B})\rvert$	(8)	[17]	Add	Invariant	Invariant	Size only	No
d_{ang_1}	$\arccos(\overline{e}_1^{\mathbb{A}} \cdot \overline{e}_1^{\mathbb{B}})$	(9)	[21]	Invariant	Linear only	Linear only	Linear only	No
d_{L2}	$\sqrt[n]{\sum_{i=1}^{3}\sum_{j=1}^{3}(\mathbb{A}_{ij} - \mathbb{B}_{ij})^n}$	(10)	[4]	Add	Smooth	Ok	All	Yes
s_{sp}	$\sum_{i=1}^{3}\sum_{j=1}^{3}\mathbb{A}_{ij}\mathbb{B}_{ij}$	(11)	[1]	Increases	Smooth	Not self-similar (1)	All	No
s_{tsp}	$\sum_{i=1}^{3}\sum_{j=1}^{3}\lambda_i^{\mathbb{A}}\lambda_j^{\mathbb{B}}(\overline{e}_i^{\mathbb{A}}\overline{e}_j^{\mathbb{B}})^2$	(12)	[7]	Increases	Smooth	Not self-similar (1)	All	No
s_{ntsp}	$\frac{s_{tsp}(\mathbb{A},\mathbb{B})}{\mathrm{tr}(\mathbb{A})\mathrm{tr}(\mathbb{B})}$	(13)	[7]	Invariant	Smooth	Not self-similar (1)	Shape and orientation only	no
s_{pnl}	$\hat{c}_l^{\mathbb{A}}\hat{c}_l^{\mathbb{B}}s_l(\mathbb{A},\mathbb{B}) + \hat{c}_p^{\mathbb{A}}\hat{c}_p^{\mathbb{B}}s_p(\mathbb{A},\mathbb{B}) + \gamma * \hat{c}_s^{\mathbb{A}}\hat{c}_s^{\mathbb{B}}s_s(\mathbb{A},\mathbb{B})$	(21)	[10]	mult	smooth	not self-similar (2)	shape and orientation only	no
d_g	$N(\mathbb{A}^{-\frac{1}{2}}\mathbb{B}\mathbb{A}^{-\frac{1}{2}})$	(15)	[4]	Mult	Smooth	Sensitive	Sensitive	Yes
d_{LE}	$\sqrt{\mathrm{tr}((\log(\mathbb{A}) - \log(\mathbb{B}))^2)}$	(17)	[2]	Mult	Smooth	Sensitive	Sensitive	Yes
d_{KL}	$\frac{1}{2}\sqrt{\mathrm{tr}(\mathbb{A}^{-1}\mathbb{B} + \mathbb{B}^{-1}\mathbb{A}) - 2n}$	(18)	[16]	Mult	Smooth	Sensitive	Sensitive	Yes
s_{Bhat}	$e^{-\frac{1}{2}ln\left(\frac{\det(\frac{\mathbb{A}+\mathbb{B}}{2})}{\sqrt{\det(\mathbb{A})\det(\mathbb{B})}}\right)}$	(19)	[6]	mult	smooth	sensitive	sensitive	yes

The ds measures that are not listed have the same properties as ds_{FA}

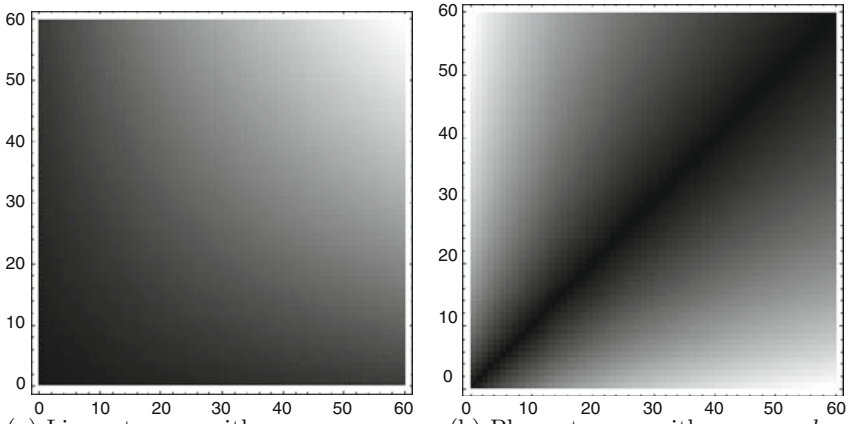

(a) Linear tensors with measure s_{tsp}. (b) Planar tensors with measure d_g.

Fig. 4. Comparison plots with tensors changing size

Measures s_{sp} and s_{tsp} have behavior as shown in Fig. 4(a). They return bigger values if the MD is larger. As a consequence, the result of comparing two tensor that are exactly the same is not constant and depends on the size of the tensor. There is no upper limit for the similarity measure that can be given. We call the behavior of the measures *increasing* in Table 2.

The remaining measures are listed as *mult*. This means that they behave as shown in Fig. 4(b). The relation between the output of the measure and the ratio $MD(\mathbb{A})/MD(\mathbb{B})$ of the size of the two tensors is linear, and (24) is valid.

6.2 Orientation

Measure d_{ang_1} only works well for tensors with linear shape. All scalar-index-based measures (ds) are invariant to rotation. All measures except ds and d_{ang_i} have similar behavior under rotation. For tensors with linear shape, they have the same behavior as d_{ang_1}, which is shown in Fig. 3(a). Results for s_{KL} for tensors with planar shape is shown in Fig. 5. The other measures show similar behavior. It is similar to that in Fig. 3(a). Except for d_{ang_i}, all measures are invariant to rotations if at least one of the two tensors that are being compared has spherical shape, that is,

$$m(\mathbb{S}, \mathbb{A}) = m(\mathbb{S}, R^T \mathbb{A} R) \tag{25}$$

for spherical tensor $\mathbb{S}$, and $\mathbb{A} \in Sym^+(3)$ and rotation R. For tensors whose shape is not purely linear, planar, or spherical, the resulting plots are a weighted average of the plots of the respective tensor types. This is shown in Fig. 6 for d_{LE}. All measures, except d_{ang_i} in the areas where its result is random, are invariant to rotations of both tensors, thus, for any rotation R

$$m(\mathbb{A}, \mathbb{B}) = m(R^T \mathbb{A} R, R^T \mathbb{B} R) \tag{26}$$

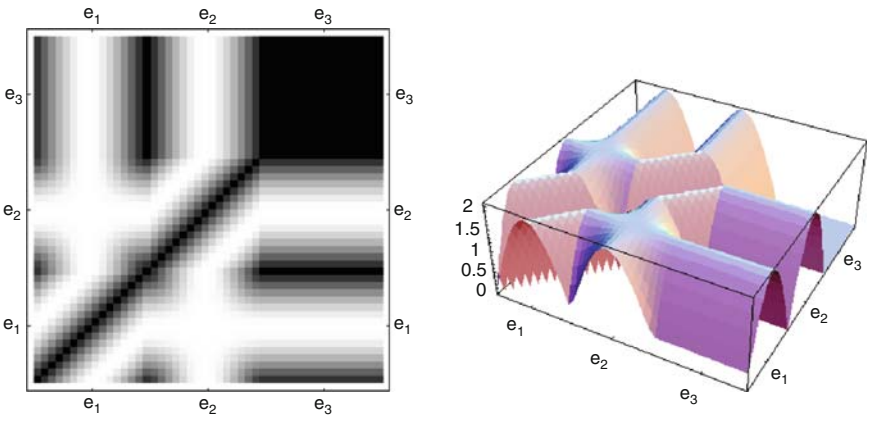

Fig. 5. Comparison plot of planar tensors rotated around λ_1, λ_2, and λ_3 for d_{KL}. See Fig. 1(b)

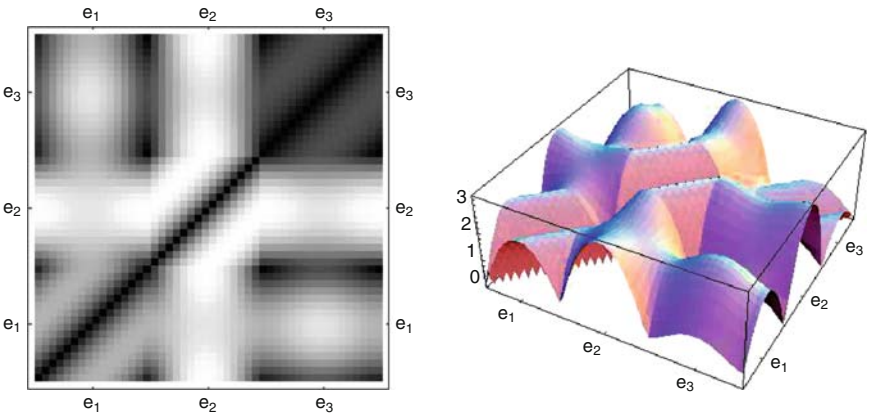

Fig. 6. Comparison plot for tensors rotated around $\overline{e}_1$, $\overline{e}_2$, and $\overline{e}_3$ for d_{LE}. The tensors do not have pure linear, planar, or spherical shape, but eigenvalues $\lambda_1 = 1.0$, $\lambda_2 = 0.5$, and $\lambda_3 = 0.1$

To refine the classification of these measures, we compared their results by computing the RMSD between them. Measures d_{L2}, d_g, d_{LE}, d_{KL}, and s_{Bhat} (since s_{Bhat} it is not a distance, we inverted the result, $d_{Bhat} = 1 - s_{Bhat}$, before the comparison) are similar to each other ($RMSD \approx 0$). We can define another subgroup with the measures s_{sp}, s_{tsp}, and s_{ntsp}. These measures give the same result, $RMSD = 0$.

6.3 Shape

Of the measures that we analyzed, only ds_{MD} is invariant to shape changes. The behavior for ds_{FA} is shown in Fig. 3(b). The other ds measures show similar behavior where tensors that differ can have a distance of zero depending on which anisotropy measure is used. d_{ang_i} can give random values depending on the shape of the diffusion. The behavior of d_{L2} is shown in Fig. 7, The diagonal is black, and the greatest distance occurs between linear and spherical tensors.

Measures s_{sp}, s_{tsp}, and s_{ntsp} all behave similar to what is shown in Fig. 8. Tensors with linear shape are very similar to themselves. However, tensors with planar or spherical shapes are less similar to themselves. Thus, the similarity between a tensor and itself depends on its shape. Because of this

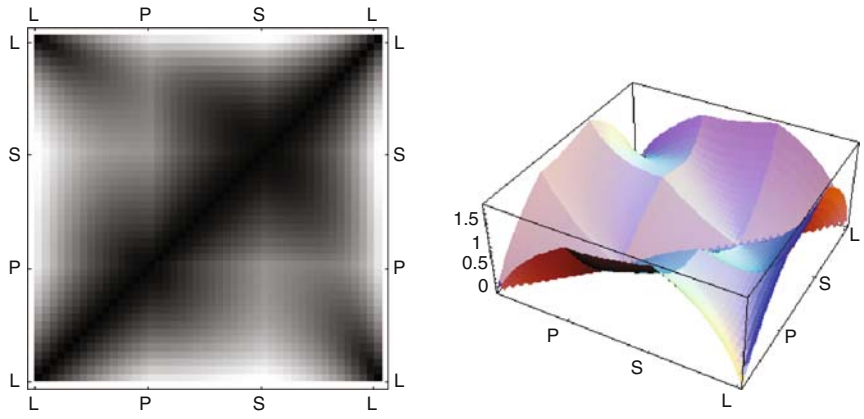

Fig. 7. Comparison plot of d_{L2} for shapes changing from linear to planar to spherical to linear

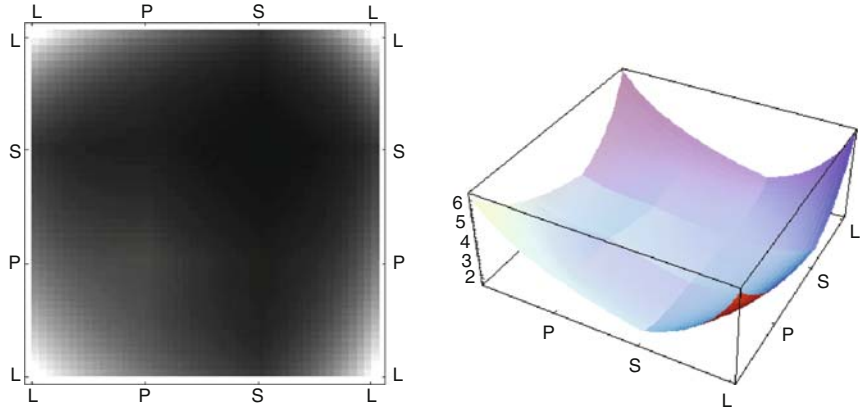

Fig. 8. Comparison plot for changing shapes for S_{tsp}

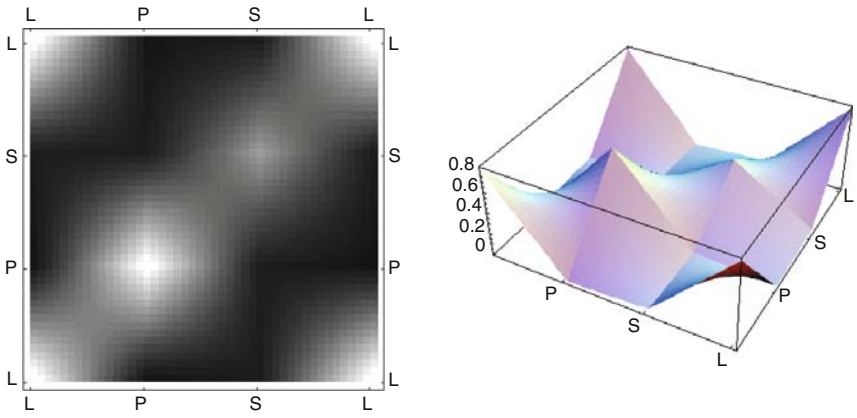

Fig. 9. Comparison plot for changing shapes for S_{pnl}

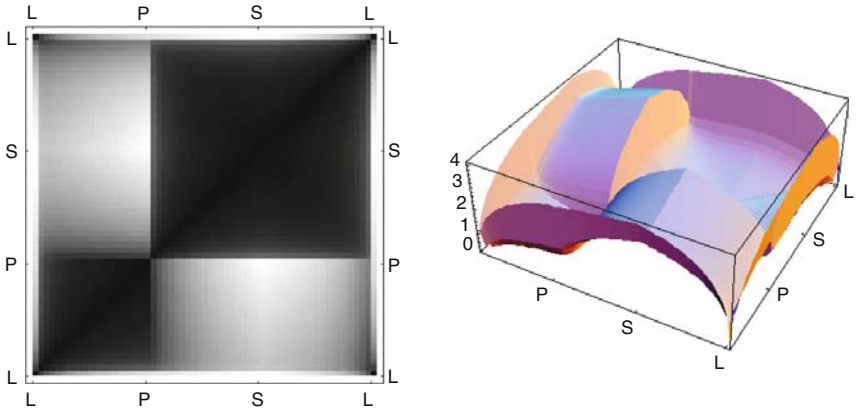

Fig. 10. Comparison plot for shapes changing from linear (L) to planar (P) to spherical (S) to linear (L). The plot shows d_{KL}. $\lambda_1/\lambda_3 = 100$ for tensors with "pure" linear and planar shape

behavior, we cannot convert these similarity measures to distance measures, which fulfill metric condition (5). We list this in Table 2 as *not self-similar (1)*.

The behavior under shape changes for s_{pnl} is shown in Fig. 9. The values on the diagonal are brighter than the values next to it because tensors are similar to themselves. However, the actual values on the diagonal are not all the same. Thus, for s_{pnl} the similarity between a tensor $\mathbb{D}$ and itself also depends on the shape of $\mathbb{D}$. We list this in Table 2 as *not self-similar (2)*.

The plots for measures based on Riemannian geometry and statistics (see Sects. 4.4 and 4.5) show steep edges in areas where at least one of the eigenvalues is very small. This is shown for d_{KL} in Fig. 10, where $\lambda_1/\lambda_3 = 100$ for

tensors with "pure" linear and planar shape. This behavior is listed as *sensitive* in Table 2. In medical data, the chance to be exactly on the very steep part is small because the fractions between eigenvalues are not that large. However, it is always possible that two similar tensors are on opposite sides of this edge, which will result in a large difference. Also, noise in medical data can change the fractions of the eigenvalues in such a way that the tensors come closer to the steep edges, that is, small variations in the shape results in large variation in the measures.

6.4 Robustness

We repeated the experiments of the previous sections after adding noise as described in Sect. 5.4 to the input tensors. The noise consists of uniformly distributed random values $\varepsilon \in [-0.01, 0.01]$, which are added to the components of the tensors. We then compare the root mean square difference (RMSD) between the output of the normalized plots with and without noise. The results are shown in Table 3. The more robust the measures are to noise, the lower the values in the table.

The shape experiments were done with tensors that have varying eigenvalues but with constant mean diffusivity, $\frac{\lambda_1+\lambda_2+\lambda_3}{3} = 1$. The eigenvalues are changed from linear ($\lambda_1 > \lambda_2 = \lambda_3$) to planar shape ($\lambda_1 = \lambda_2 > \lambda_3$), from planar to spherical shape ($\lambda_1 = \lambda_2 = \lambda_3$), and back to linear shape.

The orientation experiments were done with a linear tensor ($\lambda_1 = 1.0$, $\lambda_2 = \lambda_3 = 0.1$) that is rotated. The size experiments use the same linear tensor, which is enlarged by multiplying all components of the tensor with values from 0 to 60. The noise is added to the tensors after the changes in shape, orientation, and size were done.

In Table 2 the robustness of the measures is summarized. Some measures prove to be robust within only one or two of the invariant properties (shape,

Table 3. Root mean square difference (RMSD) between the sets of tensors with and without small variations

	Equation	Shape	Orientation	Size
ds_{FA}	(8)	0.007	0.372	0.279
ds_{MD}	(8)	0.316	0.332	0.002
d_{ang_1}	(9)	0.409	0.006	0.338
d_{L2}	(10)	0.005	0.013	0.002
s_{sp}	(11)	0.009	0.024	0.002
s_{tsp}	(12)	0.009	0.024	0.002
s_{ntsp}	(13)	0.003	0.024	0.246
s_{pnl}	(21)	0.008	0.018	0.237
d_g	(15)	0.012	0.044	0.007
d_{LE}	(17)	0.012	0.042	0.007
d_{KL}	(18)	0.013	0.056	0.007
s_{Bhat}	(19)	0.014	0.048	0.006

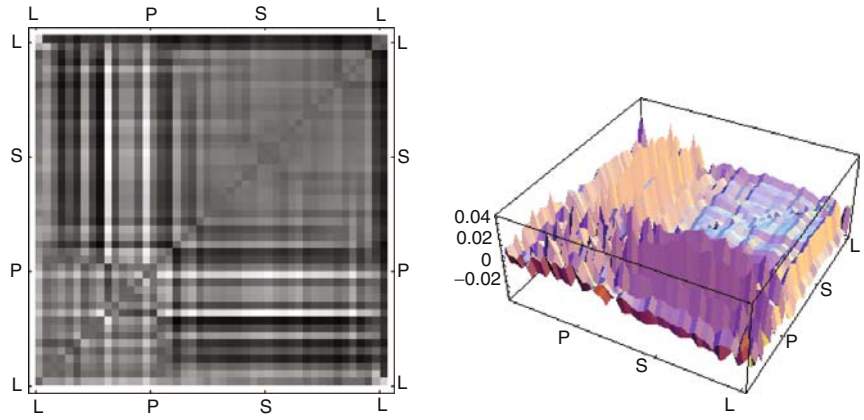

Fig. 11. Comparison plot showing the difference between the response of d_{KL} to a set with and without random noise. $RMSD = 0.013$

orientation, and size), that is, they have one or two relatively low values in Table 3. We classify them as such. For example, measure ds_{FA} is robust to changes in *shape only*. If the plots do not have steep parts, that is, high discontinuities, thus the values in Table 3 are small, we consider the noise robustness of the measures to be good for *all*.

Measure d_{L2} proves to be the most robust measure. Measure d_{ang_1} only takes the main diffusion direction into account. If the shape of the tensor is not linear, this direction can change randomly when small changes are made to the tensors. Thus, d_{ang_1} does not behave well under noise.

From the other measures, only the shape plots for d_g, d_{LE}, d_{KL}, and s_{Bhat} show steep edges. These edges appear where the shapes of the tensors are very linear or planar. Thus, in these areas the measures are very sensitive to noise. Figure 11 shows this behavior for d_{KL}.

6.5 Metric

All metrics are symmetric, this can be also seen in the plots, since they are symmetric by the diagonal.

Similarity measures have to be transformed into distance measures before we can evaluate if they are metrics. Similarity measures with *increases* as size change behavior or *not self-similar* as shape change behavior have a similarity $s(\mathbb{A}, \mathbb{A})$ that depends on the size or shape of tensor $\mathbb{A}$. Thus they cannot directly be translated into a distance measure that always fulfills metric condition (5). Measures ds, d_{ang_i}, and s_{ntsp} are invariant to one or more of the properties of Sect. 3. Thus, there are many tensors $\mathbb{A} \neq \mathbb{B}$ for which $d(\mathbb{A}, \mathbb{B}) = 0$, which invalidates metric condition (5).

It is clear that distance measures d_{L2}, d_g, d_{LE}, d_{KL} fulfill metric conditions (5) and (6). They also fulfill the triangle inequality (7) if the tensors $\mathbb{A}$ and $\mathbb{B}$

are infinitesimally close [2, 12, 16]. Therefore, they are *Riemannian metrics*. Because this is sufficient for the applications that need the distances to be a metric, we list them as *yes* for the metric property in Table 2. s_{Bhat} is a similarity measure, and so it cannot be a metric. However, it can be turned into one as is shown in [5]. Thus, we list *yes* for the metric property in Table 2.

7 Conclusions

Depending on the application, different distance or similarity measures can be used. Using the previous analysis of properties we can identify from a practical point of view the differences and similarities between the different measures.

It turns out that the behavior of s_{sp} and s_{tsp} is similar, even though s_{sp} deals with the tensor as if it is a vector. The L^2 distance d_{L2} is relatively simple, but shows good behavior. Also, all measures listed in Sects. 4.4 and 4.5 give practically the same results.

Except for s_{Bhat}, the similarity measures S cannot easily be converted into metrics, thus if that is a requirement for the application (e.g., for calculating geodesics), those measures are ruled out. This also rules out the ds measures and d_{ang_i}. Measure d_{L2} can be a good measure in that case. When using measures d_g, d_{LE}, d_{KL}, and s_{Bhat}, one has to be careful with the sensitivity to small shape changes close to the degenerate cases.

Throughout a complete brain, all diffusion properties vary. To take all properties into account when registering brains, no measure should be chosen that is invariant to any of them. Also, if the weighting for all DTs used in the registration must be the same, the similarity measures that list *increases* for size or *not self-similar* for shape should not be used because even for equal DTs, the computed similarities can vary depending on size and shape.

For interpolation of DTs the triangle inequality condition must be satisfied; therefore, only measures that are metrics can be used. Work has been done in the comparison of the different interpolation methods as in Arsigny et al. [2], Pennec et al. [12], and Kindlmann et al. [9].

We created an overview of existing distance and similarity measures for matching diffusion tensors and classified the measures. Such an overview, including recently introduced measures, was not previously available. We evaluated the properties of these measures and summed them up in Table 2. When researchers want to use a similarity or distance measure for their concrete application, they can define which properties their measure should have to and then study the measures that fulfill their requirements.

When new measures are introduced, it will be beneficial to classify them and see for which properties they differ from already existing measures, and how they differ. So in which sense they improve existing measures.

This chapter aims to help in the first selection of these measures, the next step is to test what measure performs better in a concrete application, for

example, white matter segmentation. If the goal is to segment the brain using DTs, the choice of measure depends on which properties are of importance for a given area. For example, segmenting the thalamic nuclei requires dependency of orientation for the measure used [21], while white and grey matter can be distinguished using the tensor shape.

For future work, it would be necessary to study the behavior of these measures under a more realistic model of noise. Furthermore, it would be useful to compare the measures in a concrete practical set up and see whether they behave according to our expectations. Also for some applications, such as segmentation and registration, it can prove useful to compare methods that apply the measures to the DTs directly with methods that segment or register derived data, such as fibers (the output of a fiber tracking algorithm). We also plan to use the measures for quantitative analysis and visualization of differences between tensors in small areas of the heart and brain DTI datasets. We expect that the overview of properties, that we presented in this work, will simplify the analysis of the results for these applications. It can also give indications for which properties a new measure for DTs might be useful. For example, having a measure of which the result for size changes is fractional (listed as *ratio* in Table 2), where the shape-dependency is not *sensitive*, can prove useful.

Acknowledgments

We thank Laura Astola for her insights in statistics and Riemannian geometry. This work was supported by the Dutch BSIK program entitled Molecular Imaging of Ischemic heart disease (project number BSIK 03033), Fundação para a Ciência e a Tecnologia (FCT, Portugal) under grant SFRH/BD/24467/2005, and the Netherlands Organization for Scientific Research (NWO-VENI grant 639.021.407).

References

[1] D. Alexander, J. Gee, and R. Bajcsy. Similarity measures for matching diffusion tensor images. In *Proceedings of the British Machine Vision Conference (BMVC)*, 93–102, 1999.

[2] V. Arsigny, P. Fillard, X. Pennec, and N. Ayache. Log-Euclidean metrics for fast and simple calculus on diffusion tensors. *Magnetic Resonance in Medicine*, 56(2):411–421, 2006.

[3] P.J. Basser and C. Pierpaoli. Microstructural and physiological features of tissues elucidated by quantitative-diffusion-tensor MRI. *Journal of Magnetic Resonance*, 111(3):209–219, 1996.

[4] P.G. Batchelor, M. Moakher, D. Atkinson, F. Clamante, and A. Connelly. A rigorous framework for diffusion tensor calculus. *Magnetic Resonance in Medicine*, 53:221–225, 2005.

[5] D. Comaniciu, V. Ramesh, and P. Meer. Kernel-based object tracking, *IEEE Transactions on Pattern Analysis and Machine Intelligence*, 25:564–577, 2003.

[6] R.O. Duda, P.E. Hart, and D.G. Stork. *Pattern Classification (2nd Edition)*. Wiley, New York, 2000.

[7] L. Jonasson, X. Bresson, P. Hagmann, O. Cuisenaire, R. Meuli, and J. Thiran. White matter fiber tract segmentation in DT-MRI using geometric flows. *Medical Image Analysis*, 9(3):223–236, 2005.

[8] G. Kindlmann. *Visualization and Analysis of Diffusion Tensor Fields*. PhD thesis, School of Computing, University of Utah, 2004.

[9] G.L. Kindlmann, R.S.J. Estpar, M. Niethammer, S. Haker, and C.-F. Westin. Geodesic-loxodromes for diffusion tensor interpolation and difference measurement. In N. Ayache, S. Ourselin, and A. Maeder, editors, *MICCAI (1)*, volume 4791 of *Lecture Notes in Computer Science*, pages 1–9. Springer, 2007.

[10] J. Lötjönen, M. Pollari, T. Neuvonen. Affine registration of diffusion tensor MR images. In *MICCAI 2006*, Springer, Berlin Heidelberg, pp. 629–636, 2006.

[11] E.R. Melhem, S. Mori, G. Mukundan, M.A. Kraut, M.G. Pomper, and P.C.M. van Zijl. Diffusion tensor MR imaging of the brain and white matter tractography. *American Journal of Roentgenology*, 178(1):3–16, 2002.

[12] X. Pennec, P. Fillard, and N. Ayache. A riemannian framework for tensor computing. *International Journal of Computer Vision*, 66(1):41–66, 2006.

[13] C. Pierpaoli and P.J. Basser. Toward a quantitative assessment of diffusion anisotropy. *Magnetic Resonance in Medicine*, 36:893–906, 1996.

[14] M. Rousson, C. Lenglet, and R. Deriche. Level set and region based surface propagation for diffusion tensor MRI segmentation. In *Computer Vision Approaches to Medical Image Analysis (CVAMIA) and Mathematical Methods in Biomedical Image Analysis (MMBIA) Workshop*, Prague, May 2004.

[15] A. Vilanova, S. Zhang, G. Kindlmann, and D. Laidlaw. An introduction to visualization of diffusion tensor imaging and its applications. In J. Weickert and H. Hagen, editors, *Visualization and Processing of Tensor Fields*, Mathematics and Visualization, chapter 7, Springer, Berlin Heidelberg, pp. 121–153, 2005.

[16] Z. Wang and B.C. Vemuri. DTI segmentation using an information theoretic tensor dissimilarity measure. *IEEE Transactions on Medical Imaging*, 24(10):1267–1277, 2005.

[17] C.-F. Westin, S. Peled, H. Gudbjartsson, R. Kikinis, and F.A. Jolesz. Geometrical diffusion measures for MRI from tensor basis analysis. In *ISMRM '97*, pp. 1742, 1997.

[18] H. Zhang, P.A. Yushkevich, D.C. Alexander, and J.C. Gee. Deformable registration of diffusion tensor MR images with explicit orientation optimization. *Medical Image Analysis – Special Issue: The Eighth*

International Conference on Medical Imaging and Computer Assisted intervention – MICCAI 2005, 10(5):764–785, October 2006. Invited submission. PMID: 16899392.

[19] L. Zhukov and A.H. Barr. Heart-muscle fiber reconstruction from diffusion tensor MRI. In *Proceedings of IEEE Visualization 2003*, IEEE Computer Society, pp. 597–602, 2003.

[20] L. Zhukov, K. Museth, D. Breen, R. Whitaker, and A. Barr. Level set modeling and segmentation of DT-MRI brain data, *Journal of Electronic Imaging*, 12:125–133, 2003.

[21] U. Ziyan, D. Tuch, and C. Westin. Segmentation of thalamic nuclei from DTI using spectral clustering. In *Ninth International Conference on Medical Image Computing and Computer-Assisted Intervention (MICCAI'06)*, Lecture Notes in Computer Science 4191, Copenhagen, Denmark, pp. 807–814, 2006.

http://www.springer.com/978-3-540-88377-7

Visualization and Processing of Tensor Fields
Advances and Perspectives
Laidlaw, D.H.; Weickert, J. (Eds.)
2009, XVII, 376 p., Hardcover
ISBN: 978-3-540-88377-7